

# Exploring Adsorbates of Normal and Semi-Fluorinated Alkanes on Different Substrates with Atomic Force Microscopy

Sergei Magonov, John Alexander and Sergey Belikov

SPM Labs LLC, 148 W. Orion Str. Tempe AZ 85283 USA

## Introduction

Atomic force microscopy (AFM) is a superior technique for visualization of surface nanoscale structures in a variety of samples from ultrathin adsorbates to macroscopic specimens. As force interactions between a nanoscopic tip of a cantilevered probe and sample surface are employed for such visualization, the force level and type of force detection are essential features of the technique. Keeping the tip-sample forces low is beneficial for AFM studies of soft samples. Such measurements are routinely accomplished with amplitude modulation with phase imaging (AM-PI) mode historically introduced as tapping mode [1]. A drop of the amplitude of AFM probe driven in its resonant oscillation is used as a measure of periodical tip-sample force interactions in this mode. The fast intermittent contact limits a development of plastic deformation and reduces lateral force helping to avoid sample damage. Yet the correlation between the tip forces and amplitude change is not trivial, and the effective tapping force depends not only of the value of amplitude and its set-point but also on sample elastic modulus [2]. This brings complications for regulating imaging force and performing quantitative AFM measurements. The related effects might obscure the interpretation of height and phase images commonly recorded in this mode. In the following, examples of AFM studies of ultra long alkanes ( $C_{242}H_{486}$ ) and semi-fluorinated alkanes [ $CF_3(CF_2)_{14}(CH_2)_{20}CH_3$ ] - F14H20 adsorbates on HOPG and Si substrates at different imaging conditions are discussed. In addition to visualization of the structural organization of the adsorbates we were considering several peculiarities of imaging soft layers with periodical features. Effects of tip-force, contrast variations of height images, which were also noticed earlier [3-4], and appearance of Moiré patterns in AFM images will be of prime interest.

## Experimental

### *Samples and preparation*

Samples of ultra long alkane  $C_{242}H_{486}$  and semi-fluorinated alkane F14H20 were kindly provided by Profs. G. Ungar (Sheffield, England) and M. Moeller (Aachen, Germany). The AFM specimen of  $C_{242}H_{486}$  was made by spin casting its diluted solution in toluene on freshly cleaved highly oriented pyrolytic graphite (HOPG). The atomically smooth graphite surface is characterized by tri-fold symmetry of honeycomb pattern that accommodate normal alkane molecules and their flat-lying lamella in similar regularity [5]. We were making samples of normal alkanes on HOPG with flat-lying lamellae by spin-casting of their diluted solution in toluene, which is followed by their heating to 30-40 degrees above bulk melting temperatures and final slow cooling to room temperature. This procedure results in melting of alkane material tailed by its spreading on the substrate. A gradual cooling of alkane melt to room temperature initiates an adsorbate dewetting that leads to a formation of raised crystalline aggregates, which are visualized with an optical microscope. The aggregates are surrounded by flat regions with layers of flat-lying lamellar structures. At such locations we have observed  $C_{242}H_{486}$  lamellar

arrangements. The width of the individual  $C_{242}H_{486}$  lamella is typically determined by the alkane length (~28 nm) in fully extended all-trans conformation. A tilt of the molecules inside the lamellae will reduce its width.

In earlier AFM studies of F14H20 specimens the samples were made by spin-casting of diluted solution of perfluorodecalin on different substrates [6-7]. In our study we applied a solvent-free deposition of F14H20 on Si and freshly cleaved graphite surfaces by sublimation the compound in air at high temperature. In this method the substrates were placed upside down ~0.5 cm above a thick deposit of F14H20, which was heated to 100°C. The layers of the semi-fluorinated alkane of different thickness were deposited by varying sublimation time from 35 minutes to 2 hours. In addition to the samples, we have examined thick F14H20 layer on Si, which was prepared by hot pressing the material crystalline powder between two Si plates at 140°C (40 degrees above F14H20 melting temperature). After cooling this specimen to room temperature one plate was removed, and the opened surface was examined with AFM. Thickness of the melt-crystallized F14H20 layer was several microns.

#### *AFM measurements*

AFM studies were performed in air with MultiMode microscope (Bruker), which was operated with Phoenix controller (SPM Labs). The measurements were made in contact mode and in AM-PI mode. Several types of Si and Si/Si<sub>3</sub>N<sub>4</sub> (Si tip, Si<sub>3</sub>N<sub>4</sub> lever) probes (Applied Nanostructures) were used in our studies and their resonant frequency  $\omega_{res}$ , spring constant  $k$  and inverse optical sensitivity ( $IOS$ ) were determined with Thermal Tune procedure implemented in the controller [8]. For contact mode experiments we applied Hydra 2R-100 (length/width/thickness - 100/35/0.2) probe with  $\omega_{res} = 7.0$  kHz,  $k = 3.98$  mN/m,  $IOS = 92.81$  nm/V. AM-PM studies were conducted mainly with CGS30 (190/30/1) probe with  $\omega_{res} = 49.02$  kHz,  $k = 0.559$  N/m and  $IOS = 190$  nm/V. For a comparison we used two softer CGS10 (225/30/1) probes with  $\omega_{res} = 16.6$  kHz,  $k = 140$  mN/m and  $\omega_{res} = 33.12$  kHz,  $k = 302$  mN/m; as well as stiffer probe NSG 01 (125/30/2) with  $\omega_{res} = 106.7$  kHz,  $k = 1.93$  N/m. In most experiments we applied free probe amplitudes  $A_0 = 5-10$  nm and set-point amplitudes  $A_{sp} = 0.9-0.7 A_0$ , and the images with 512×512 format were collected in most experiments. Scanning rates of 0.6-0.8 Hz were used for areas of several microns on side, and 1 Hz rate was applied for sub-micron imaging. The image treatment and analysis was performed with MountainsMap® software by Digital Surf (France).

#### **Results and Discussion**

The height image of  $C_{242}H_{486}$  adsorbate (**Fig. 1a**), which was recorded in contact mode, shows an extended terrace of one of crystalline HOPG grains. Its flat surface is decorated with strips of alkane domains oriented perpendicular to the grain boundaries. Several raised structures are noticed along the edges. These boundaries separate the grain from the neighboring ones visible in the top left and bottom right corners of the image. Few raised nanoscale crystals of the alkane are seen at the top left. They are located at periphery of a large crystalline aggregate formed during the sample preparation. The lower grain at the bottom right is decorated with domains, which are oriented differently than those in the image center. This difference leads to dissimilarity of the domains' contrast in lateral force imaging (not shown here). The observed  $C_{242}H_{486}$  adsorbate is rather fragile as the contact mode imaging at minimal force of ~0.1 nN with the soft probe ( $k = 3.98$  N/m) has damaged the surface at scans of 5  $\mu\text{m} \times 5 \mu\text{m}$

and smaller. The increase of effective tip-sample forces with the downsizing the image area, which happens due to boost of time the probe spends at sample locations, is common for most AFM modes.

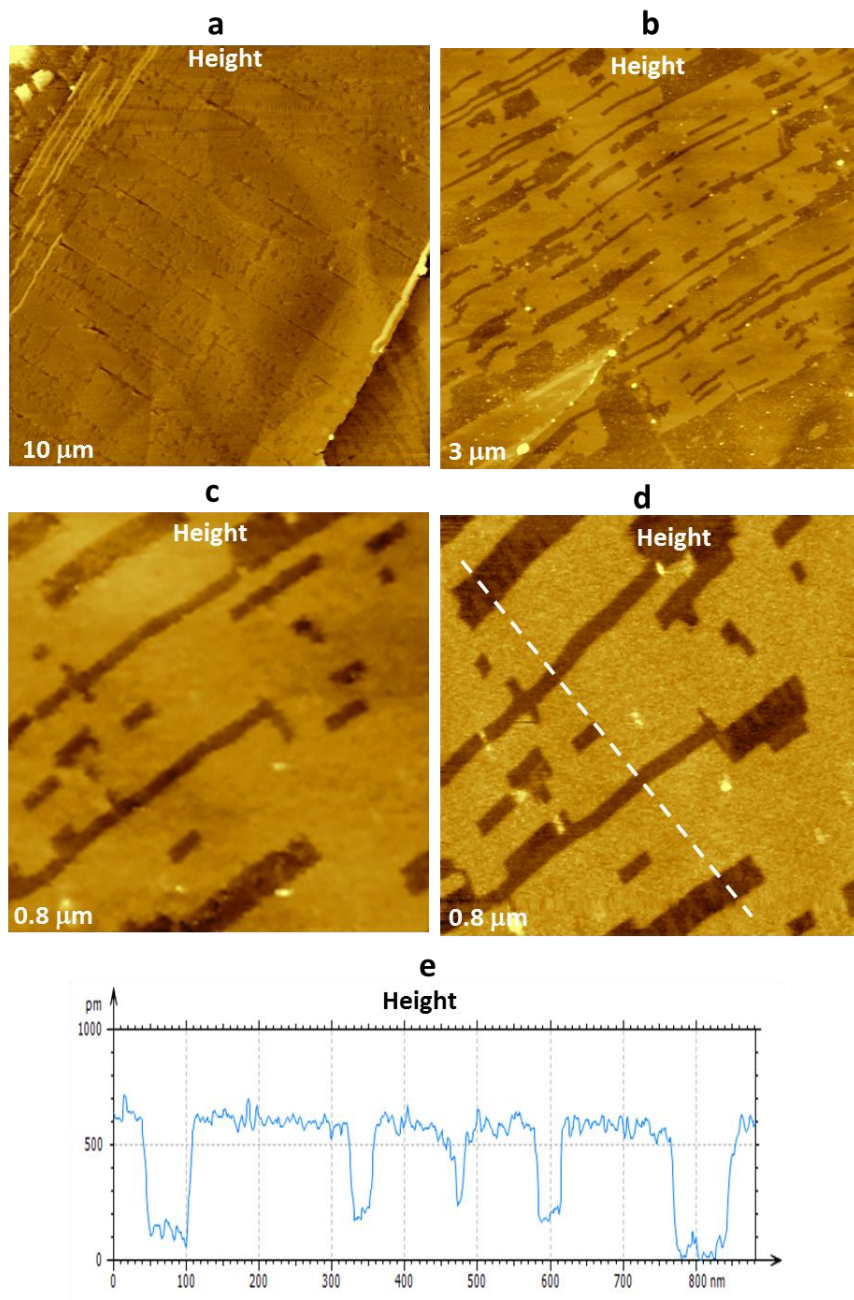


**Figure 1.** (a) Height image of  $C_{242}H_{486}$  layer on graphite in contact mode with  $Si_3N_4/Si$  probe ( $k = 3.98\ \text{mN/m}$ ). The tip force was  $0.1\ \text{nN}$ . (b) Height image of  $C_{242}H_{486}$  layer on graphite obtained in AM-PI mode with Si probe ( $k = 140\ \text{mN/m}$ ). (c) A zoomed part of the image in (b). (d) Height image of the same area as in (c), which was obtained in AM-PI mode with Si probe ( $k = 140\ \text{mN/m}$ ). (e) A cross-section curve along a direction, which was indicated in (d) with a white dashed line. The images in AM-PI mode were made with  $A_0 = 10\ \text{nm}$  and  $A_{sp} = 7\ \text{nm}$ .

Having in mind the fragile nature of the alkane adsorbate we have initiated imaging of the sample in AM-PI mode with rather soft Si probe ( $\omega_{\text{res}} = 16.6$  kHz;  $k = 140$  mN/m). Typically, much stiffer probes are applied in this mode in air that are needed to overcome the tip-sample adhesive and capillary forces disturbing stable tapping. Most likely, the hydrophobic nature of the alkane sample and low air humidity in our lab in Arizona are the factors that allowed the use of this probe on the  $\text{C}_{242}\text{H}_{486}$  surface. Height images obtained in AM-PI experiments are shown in **Fig. 1b-d**. At large scale the sample surface exhibits two layers with the top one having multiple depressions extended in the direction of a step edge between two graphite grains, **Fig. 1b**. There are also numerous white spots representing the disordered alkane particles. A zoomed part of this image is shown in **Fig. 1c** for a comparison with the height image, which was recorded on this smaller area (**Fig. 1d**). There are obvious differences in these patterns as the small scan image exhibits an increased number of rectangular dark strips. They can be assigned to missing individual lamella and lamellar assemblies, which were removed from the top layer by a scanning probe. This judgment is supported by the strips' dimensions, whose depth is consistent with the thickness of the individual alkane chains ( $\sim 0.5$  nm) and the smallest width coincides with the lamella width ( $\sim 28$  nm), **Fig. 1e**. The top surface shown in height images is smooth with undistinguished interlamellar boundaries. This might be a consequence of relatively gentle imaging that is also hinted by featureless phase images (not shown here). Nevertheless, at these imaging conditions the alkane lamellae were partially removed from the top layer.

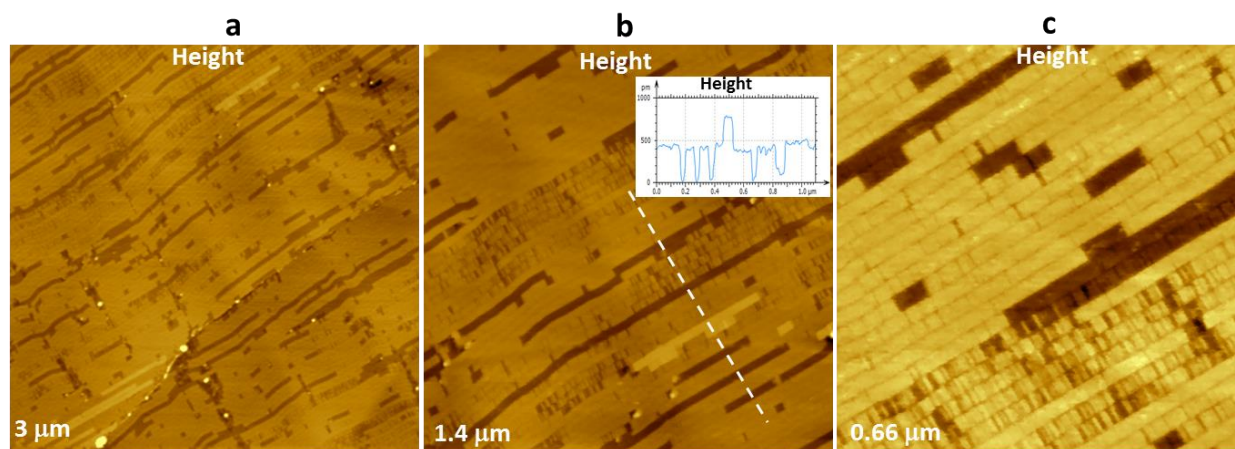


**Figure 2.** (a) Height image of  $\text{C}_{242}\text{H}_{486}$  layer on graphite obtained in AM-PI mode on the same surface area as in **Fig. 1b**. The smaller regions of this area were imaged and are shown in (b)-(c). The insert in (b) presents the height cross-section along the direction, which is marked in the image with a white dashed line. The images were obtained using Si probe with  $k = 1.93$  N/m.

The influence of the tip-force on height images of  $\text{C}_{242}\text{H}_{486}$  adsorbates was further recognized in the experiments with a much stiffer Si probe ( $\omega_{\text{res}} = 106.7$  kHz,  $k = 1.93$  N/m). The height image, which was recorded with this probe (**Fig. 2a**) shows the same area, which was examined with the soft probe, **Fig. 1b**. Overall, the image in **Fig. 2a** is free of small debris, which is seen in **Fig. 1b**. Presumably, they were brushed away by the stiffer probe. The most pronounced changes, which were caused by stronger tip-sample forces, relate to the observations of lamellar boundaries, new defective regions and appearance of several overlaying lamellar ribbons. These features are noticeable in the large scale image in **Fig. 2a**

and they are well pronounced in smaller size images in **Fig. 2b-c**. There are a large number of surface regions, in which lamellar ribbons became broken into small domains in the result of scanning with the stiff probe. The same regions were left intact in the imaging with the soft probe. The assignment of the observed structures to individual  $C_{242}H_{486}$  lamellae is supported by their width ( $\sim 28$  nm) and thickness ( $\sim 0.5$  nm), which is revealed in the insert of **Fig. 2b**.

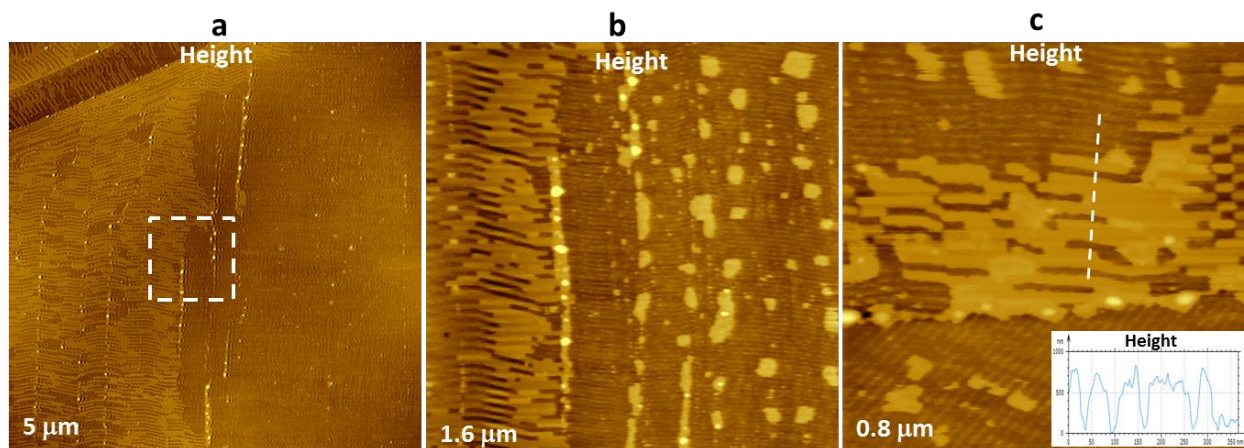


**Figure 3.** (a) Height image of  $C_{242}H_{486}$  layer on graphite obtained in AM-PI mode on another surface area. (b) Height image of a smaller location, which is marked in (a) with a white dashed square. The insert in (c) presents the height cross-section along the direction, which is marked in the image with a white dashed line. The images were recorded using Si probe with  $k = 0.559$  N/m.

The imaging of  $C_{242}H_{486}$  adsorbates with another Si probe ( $\omega_{res} = 49.02$  kHz,  $k = 0.559$  N/m) is illustrated by **Fig. 3a-c**. The largest part of height image in **Fig. 3a** presents a HOPG grain, whose left top part of the surface is covered with multiple wavy strips generally oriented in the horizontal direction. The width of these strips ( $\sim 28$  nm) correlates with the  $C_{242}H_{486}$  lamellar width. The vertical bright strips, most likely, represent the linear grain defects decorated with small patches of the alkane. Close to the grain boundary the lamellae became aligned parallel to the edge. In the left top corner of the image one can see the differently oriented lamellar structures on the neighboring grain. The right part of **Fig. 3a** is dominated by a lower adsorbate layer with multiple strips presenting the lamellar borders. They are well resolved in **Fig. 3b**, which magnifies the area marked in **Fig. 3a** with a white dashed square. The lower layer can be assigned to a tightly-packed lamellar arrangement, in which the horizontal white strips with  $\sim 28$  nm pitch represent the raised interlamellar borders formed by alkane  $-CH_3$  end groups. Multiple adsorbate domains, which are randomly spread on top of this layer, differ from the wavy lamellae and lamellar aggregates on the left. The wavy structures mimic the similar lamellar arrangement underneath. A slight shift of the neighboring alkane chains inside the lamellae explains its wavy appearance. Another surface location in **Fig. 3c** shows a boundary region where the lamellar arrangements correspond to two different crystalline orientations of the substrate. A top layer is only partially filled with lamellar structures in the region with horizontal strips' orientation. The step between the layers, which is shown in the insert of **Fig. 3c**, is close to 0.5 nm – thickness of  $C_{242}H_{486}$  molecules. The observed epitaxial arrangement of the alkane molecules, which have formed lamellar layers in immediate vicinity of HOPG surface, is quite similar to the surface order, which was earlier observed for

adsorbates of another ultralong alkane  $C_{390}H_{782}$  [9]. The outstanding challenge in visualization of weakly-bonded structures whose traces were observed in the images of  $C_{242}H_{486}$  layers, **Fig. 4a, c**.

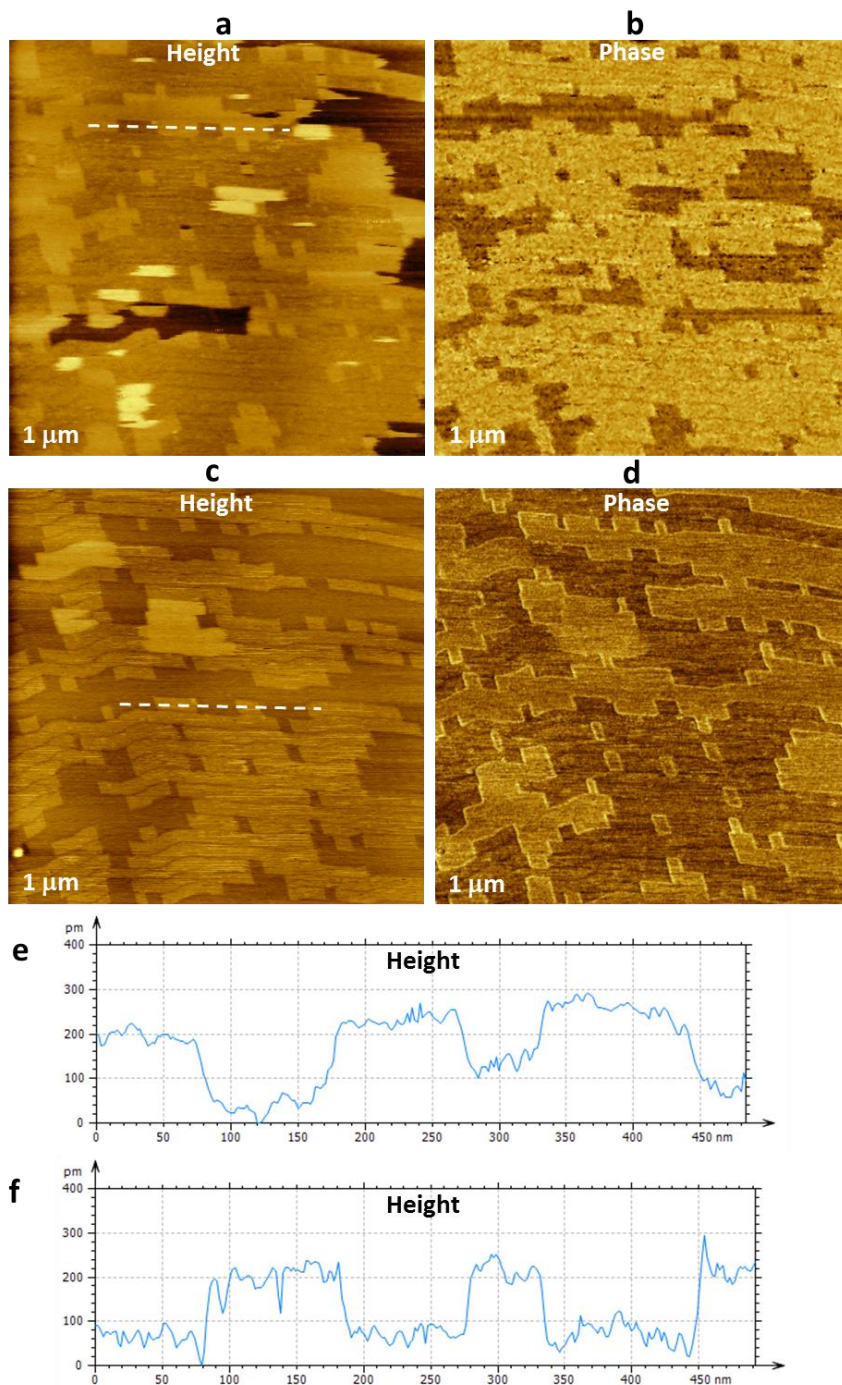


**Figure 4.** (a)-(b) Height and phase images of  $C_{242}H_{486}$  adsorbate on graphite obtained in AM-PI mode. The images were obtained in the initial scan at this area. The height in phase images in (c)-(d) were obtained at the same area after a sequence of 10 scans was accomplished. The height cross-sections in (e) and (f) were taken across the direction shown in (a) and (c) with a white dashed line.

In studies of  $C_{242}H_{486}$  adsorbates we also came across two specific AFM observations. First one is related to visualization of weak-bonded surface structures, and second one concerns accuracy of height measurements of ultrathin features in AM-PI mode [3-4]. The height and phase images of one of  $C_{242}H_{486}$  locations, which were recorded at different forces, are shown in **Fig. 4a-d**. The initial height and phase images (**Fig. 4a**), were obtained using the probe ( $k = 0.559$  N/m) with  $A_0 = 10$  nm and  $A_{sp} = 8$  nm. This area was scanned continuously more than 10 times and  $A_{sp}$  has changed to 7.5 nm. The final images in **Fig. 4c-d** exhibit a number of differences compared to the initial ones. The original surface arrangement according to the image contrast (**Fig. 4c**) can be described by several lamellar layers. The main layer is built of closely-packed lamellae, and their faint-seen borders are oriented horizontally. This layer had several vacant spots that exhibit a dark contrast, **Fig. 4a**. The layer has also multiple top domains, which are the small parts of lamellae and their in-plane aggregates. The brightest features are alkane blocks or their smaller parts. Structural transformations observed during continuous scanning have led to a better ordered lamellar arrangement. The vacancies in the main bottom layer were filled with alkane material and the layer became complete. A number of top lamellar structures have increased, and second layer has developed an epitaxial pattern mimicking the underlying lamellar arrangement. During scanning the top weakly-bonded structures have continuously changed their size and location being pushed around by the probe. Finally the mobile molecules have incorporated in to the second layer. They also have formed several lamellar ribbons of third layer seen in the top left of **Fig. 4d**. The phase contrast in **Fig. 4b** has a binary character by differentiating the structures of two main layers only. The presence of the contrast indicates a difference of the tip-sample forces at these layers.

A remarkable feature is the reverse of the height and phase contrast in **Fig. 4c-d** caused by lowering of  $A_{sp}$ . The height cross-sections along the same direction, which is indicated with the white dashed line in **Fig. 4a, c**, are compared in **Fig. 4e, f**. The evident change of height corrugations, which are in 200 pm – 300 pm range, complicates the image interpretation. The height of the top lamellar layer, which was measured in AM-PI mode with the soft probe, is around 0.5 nm that correlates well with the width of alkane molecule in all-trans conformation. This suggests that the alkane “zigzag” chains in surface layer are vertically oriented. The corrugations in **Fig. 4a, c** are smaller and correlate with the height of the “zigzag” chain lying flat. However, the question about what height image represents true topography is opened. The problem is that the tip-sample force interactions are shifting a probe resonance and lowering its quality factor both influencing the probe amplitude. These effects are reflected in height and phase image of  $C_{242}H_{486}$  adsorbates.

Prior to a consideration of AFM data obtained on F14H20 adsorbates it is important to notice that in this molecule, which extends to 4.85 nm in length, the hydrogenated part adopts the all-trans conformation and the perfluorinated sequence implements helical conformation. This leads to difference in cross-sections of  $-(CF_2)_{14}-$  chain ( $28.3\text{\AA}^2$ ) and  $-(CH_2)_{20}-$  chain ( $18.5\text{\AA}^2$ ). This dissimilarity and incompatibility of the segments govern F14H20 packing motifs in their various self-assemblies (spirals, toroids, ribbons and their intermediates) on different substrates and in diverse vapor environments. Several issues of the image interpretation were encountered in studies of F14H20 adsorbates on HOPG. A sublimation of this compound for 25 minutes has resulted in deposition of F14H20 particles at the edges of graphite terraces and a formation of domains scattered over HOPG surface. One such domain, which is almost invisible in the height image, is recognized by a dark contrast in phase image, **Fig. 5a-b**.

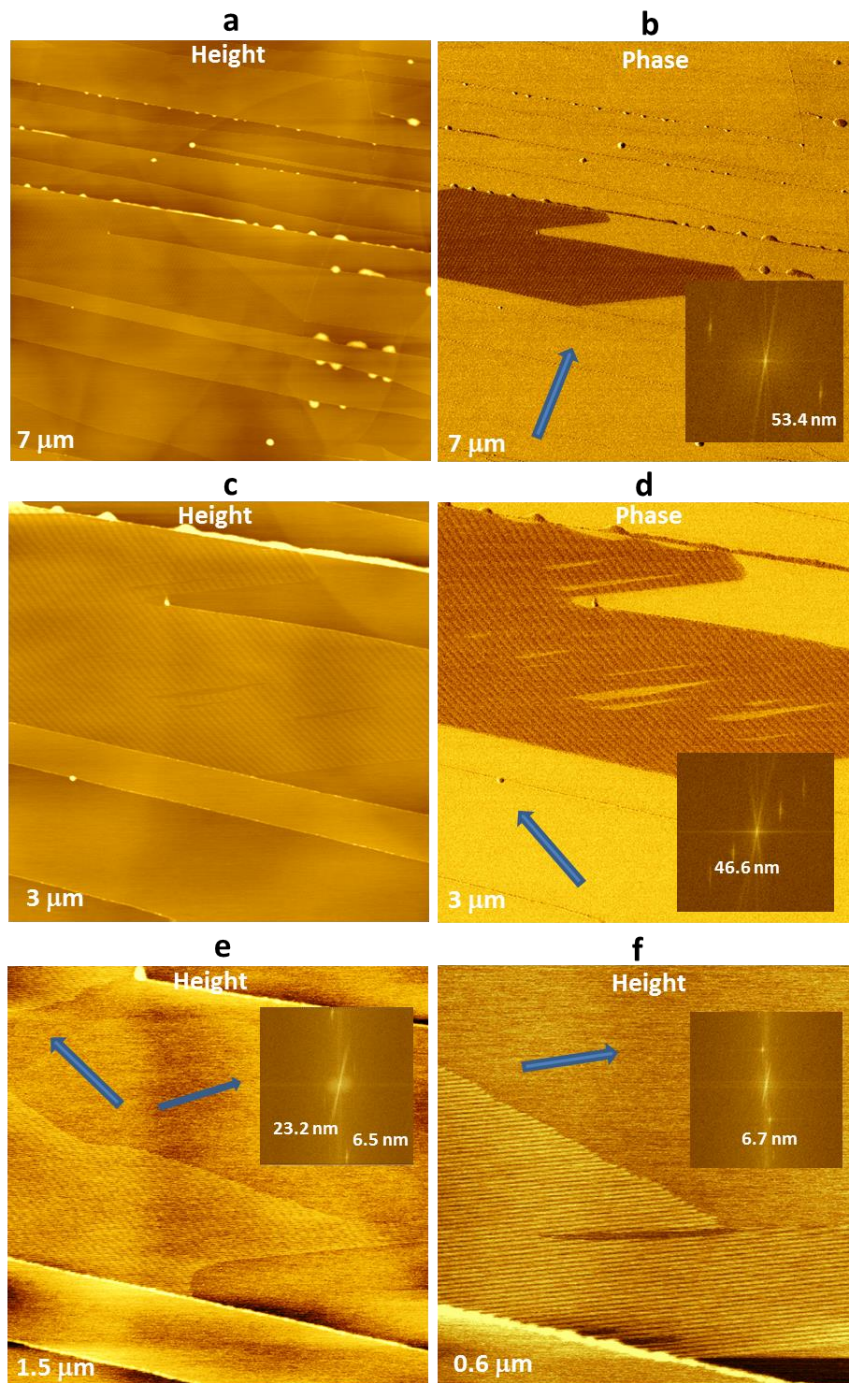


**Figure 5.** (a)-(b) Height and phase images of the F14H20 adsorbate on graphite obtained in AM-PI mode. The adsorbate was prepared by 25 min. sublimation. Inside (b) there are the PSD plot with the main spacing of the striped pattern, and the blue arrow that shows the strip direction. (c)-(d) Height and phase images of a part of the area shown in Fig. 5a-b. Inside (c) there are the PSD plot with the main spacing of the striped pattern, and the blue arrow that shows the strip direction. (e)-(f) Height and phase images of a part of the area shown in Fig. 5c-d. Inside (e) there are the PSD plot with the two spacings of the image patterns and two blue arrows, which show the direction of two striped structures. Inside (f) there are the PSD plot with the main spacing of the striped pattern, and the blue arrow that shows the strip direction. The images were recorded using Si probe with  $k = 0.559$  N/m.

The domain exhibits a striped nanostructure whose size and orientation is also indicated by power spectrum density (PSD) plot in the insert of **Fig. 5b**. According to this plot the periodical structures have a pitch 53.4 nm and their orientation is indicated with a blue arrow. As the imaging area was reduced, **Fig. 5c-d**, the domain has started to show vacancies, which are likely due to a partial removal of the adsorbate by scanning probe. The orientation and pitch of periodical structures, which are seen well in height and phase images, have changed. The pitch became 46.6 nm and the orientation, which is marked with a blue arrow in **Fig. 5d**, substantially differs from one in **Fig. 5b**. Scanning on a smaller area has intensified a removal of the adsorbate, and the domain size has reduced substantially, **Fig. 5e**. The strips of 23.2 nm apart are distinguished in this height image. There are also strips with much smaller spacing of 6.5 nm, which are barely seen in the image but obvious in PSD plot in the insert. The orientations of these strips are shown with the thick and thin blue arrows, respectively. The height image of a sub-micron area in **Fig. 5f** shows a remained part of F14H20 adsorbate with a pitch of 6.5 nm. Only few periodical features with the same pitch were found in the image of 250 nm (not shown here). The height step between the top of periodical features and the flat substrate is in the 300-400 pm range. These observations can be explained by Moire effects caused by combination of periodic image features and 512 scanning lines of the images. True periodical features, which are related to the lamellae of F14H20, were recorded in the sub-micron images. Their width of 6.5 nm is consistent with Bragg spacing found in X-ray experiments [10]. This value is larger than the length of the individual molecule but it is consistent with lamellar model having a bilayer arrangement of the tilted parallel or tilted antiparallel packing of the semi-fluorinated molecules.

The observed gradual removal of single F14H20 layer took place in imaging applying CGS30 probe with  $k = 0.559$  N/m. A more gentle study was performed at other sample location with CGS10 probe with  $k = 302$  mN/m. Height and phase images of this region (**Fig. 6a-b**) show not only ultrathin patches, which are best recognized by a dark phase contrast, but also thicker adsorbate domains. A part of this location is shown in height image, **Fig. 6c**, which was recorded as 256×256 pattern. The bottom of the image and top left corner show the stripes with a pitch of 27.3 nm, as detected by PSD plot placed in the insert of the image. This is another example of Moire pattern, which has changed to a periodical structure with smaller pitch in the 512×512 image recorded at the same spot. As in the previous example, a true periodical arrangement of F14H20 lamellae was recorded in the sub-micron images, **Fig. 6d**. The spacing of the lamellar layer of 6.5 nm, which is extracted from PSD plot in **Fig. 6e**, is identical to one obtained of the previous sample. The height of the layer, which is seen from the height cross-section (**Fig. 6f**) across the direction shown with a white dashed line in **Fig. 6d**, suggests that this is a double lamellar layer. Two bright ribbons, which are overlaying two lamellae each, are thinner (~0.3 nm) and can be assigned to pairs of individual lamellae with flat-lying molecules.

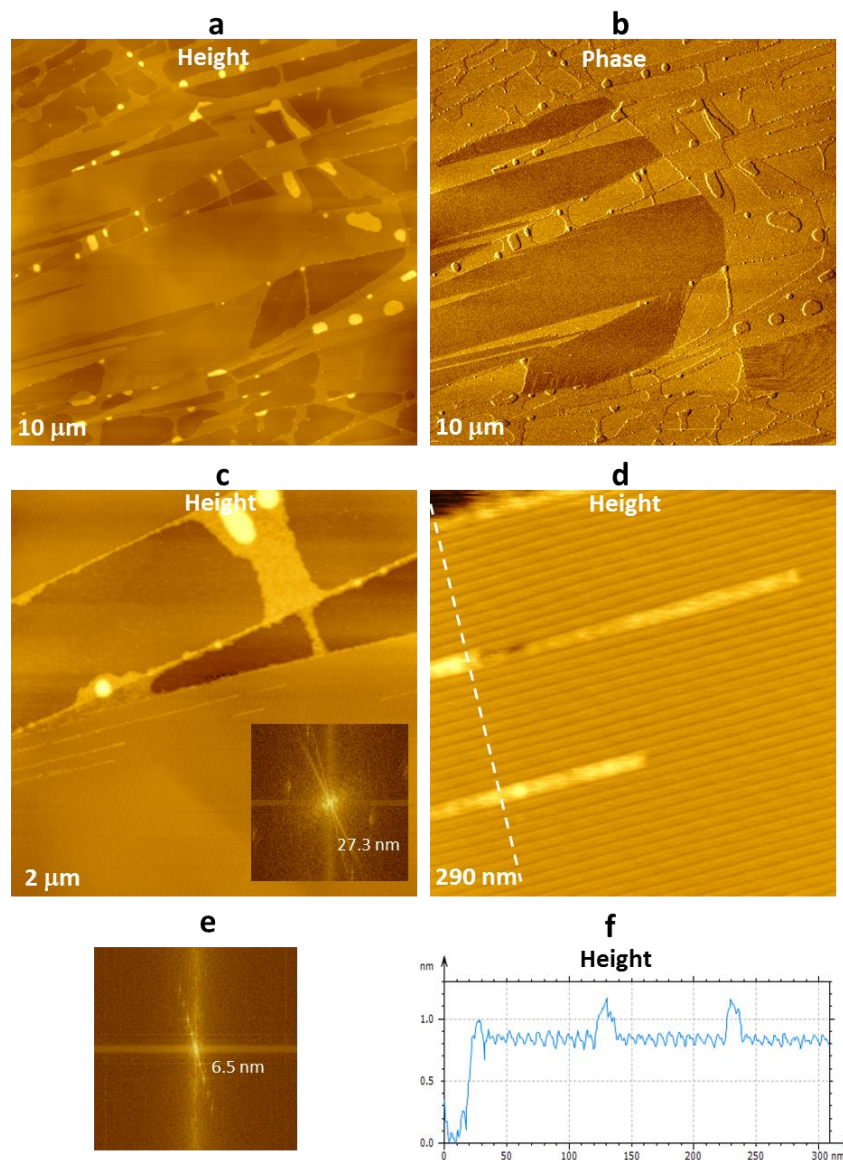


**Figure 6.** (a)-(b) Height and phase images (AM-PI) mode of another location of F14H20 adsorbate on graphite, which was prepared by 25 minutes sublimation. (c)-(d) Height images of smaller parts of the area shown in **Fig. 5a-b**. The insert in (c) shows the PSD plot and the main spacings of the striped structure. The PSD plot and the height cross-section, which was taken along the direction shown in (d) with a white dashed line, are presented in (e) and (f). The images were recorded using Si probe with  $k = 0.302$  N/m.

The problem of the image contrast reversal was noticed in imaging of thicker F14H20 adsorbate on HOPG, which were deposited on the substrate by 2 hour sublimation. The height and phase images, which were obtained in AM-PI mode with the Si probe (190/30/1) at low tip-force, are shown in **Fig. 7a-b**. The graphite steps are decorated with the bright patterns of F14H20 droplets whose horizontally extended shapes confirm a gentle profile tracking. A domain with linear stripes exhibits a weak dark contrast in height image. The same features, which can be assigned to F14H20 ribbons, are well defined in the phase image. This imaging was not very stable, and in the next scan in vertical direction a sharp

change of height and phase contrast of the ribbons assembly to bright one had happened, **Fig. 7c-d**. The contrast was stable as the set-point amplitude was slightly reduced, **Fig. 7e-f**. The observed dark contrast of the assemblies, which are seen as the 1 nm deep depressions in the substrate **Fig. 7a**, is a pure effect of dissimilar tip-sample forces at the adsorbate and substrate locations. In the higher force images the assembly has height around 2 nm.

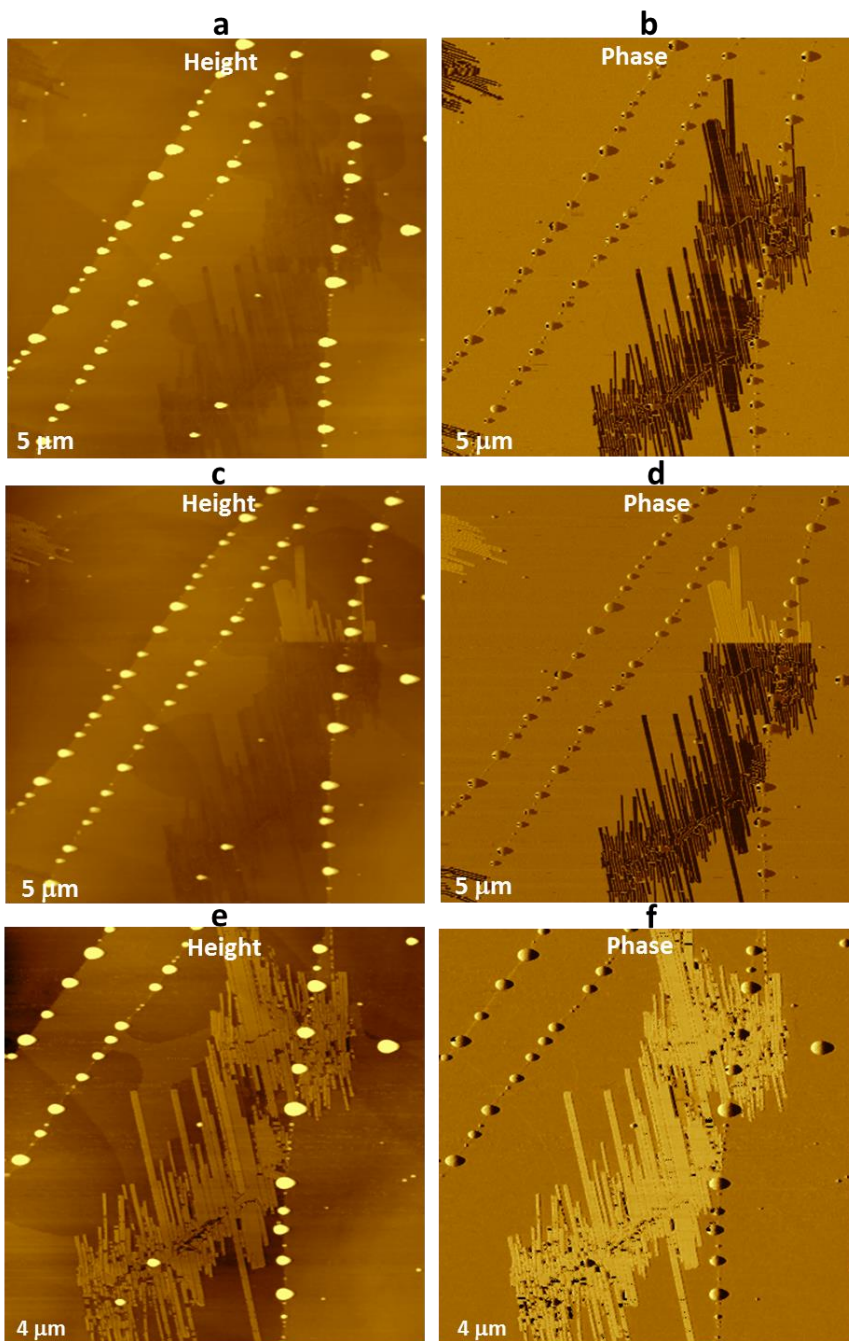


**Figure 7.** Height and phase images of the F14H20 ribbons' assembly, which was deposited on HOPG by sublimation during 2 hours. AM-PI mode with Si probe ( $k = 0.302$  N/m) was applied. The images in (a)-(b) and (c)-(d) were recorded at  $A_0 = 10$  nm and  $A_{sp} = 8$ . The images in (e)-(f) were obtained at  $A_0 = 10$  nm and  $A_{sp} = 6$  nm.

The height images in **Fig. 8a-b** show fine structural features of the flat ribbons forming the assembly.

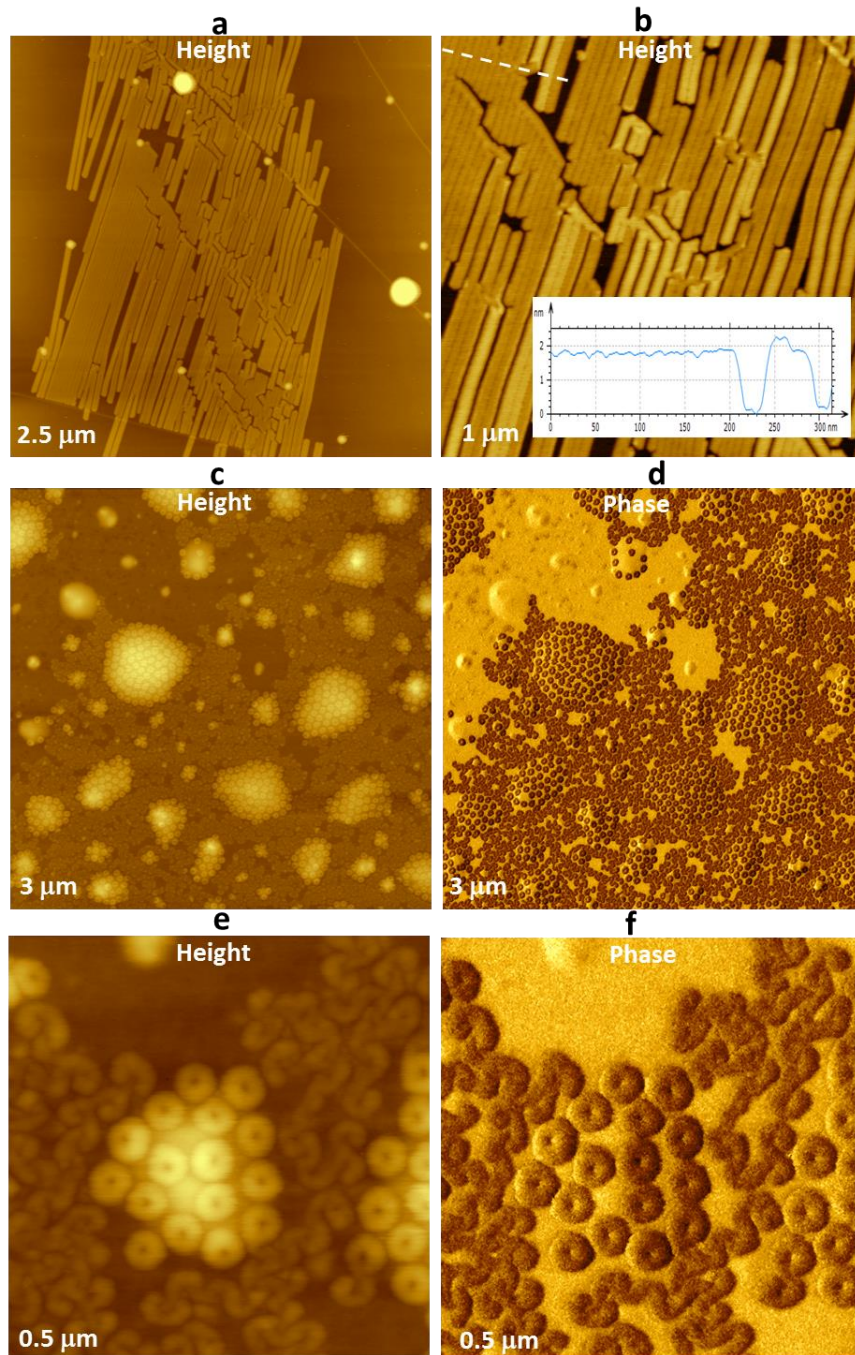


**Figure 8.** Height and phase images of the F14H20 ribbons' assembly on HOPG (a)-(b), and F14H20 adsorbate on Si (c-f), obtained by 2 hours sublimation. AM-PI mode with Si probe ( $k = 0.302 \text{ N/m}$ ) was applied at  $A_0 = 10 \text{ nm}$  and  $A_{sp} = 6 \text{ nm}$ . The insert in (b) shows the cross-section along the direction marked with a white dashed line.

The ribbons have different width in the range from 17.2 nm to 40.6 nm. The smallest are less than 2 nm and the larger ones are slightly higher, see the insert in **Fig. 8b**. As compared to HOPG, a sublimation of F14H20 adsorbates was less efficient on Si substrate and inferior on mica. After 2 hours sublimation

the Si surface was almost completely covered with self-assemblies of two kinds, **Fig. 8c-d**. They can be described as spirals and toroids, and a distinct phase contrast indicated their softness compared to the substrate. The size of the self-assemblies was estimated in **Fig. 8e-f**. The toroids are ~3 nm in height and 45-53 nm in diameter. The spirals are twice smaller in height and their width is ~20 nm.

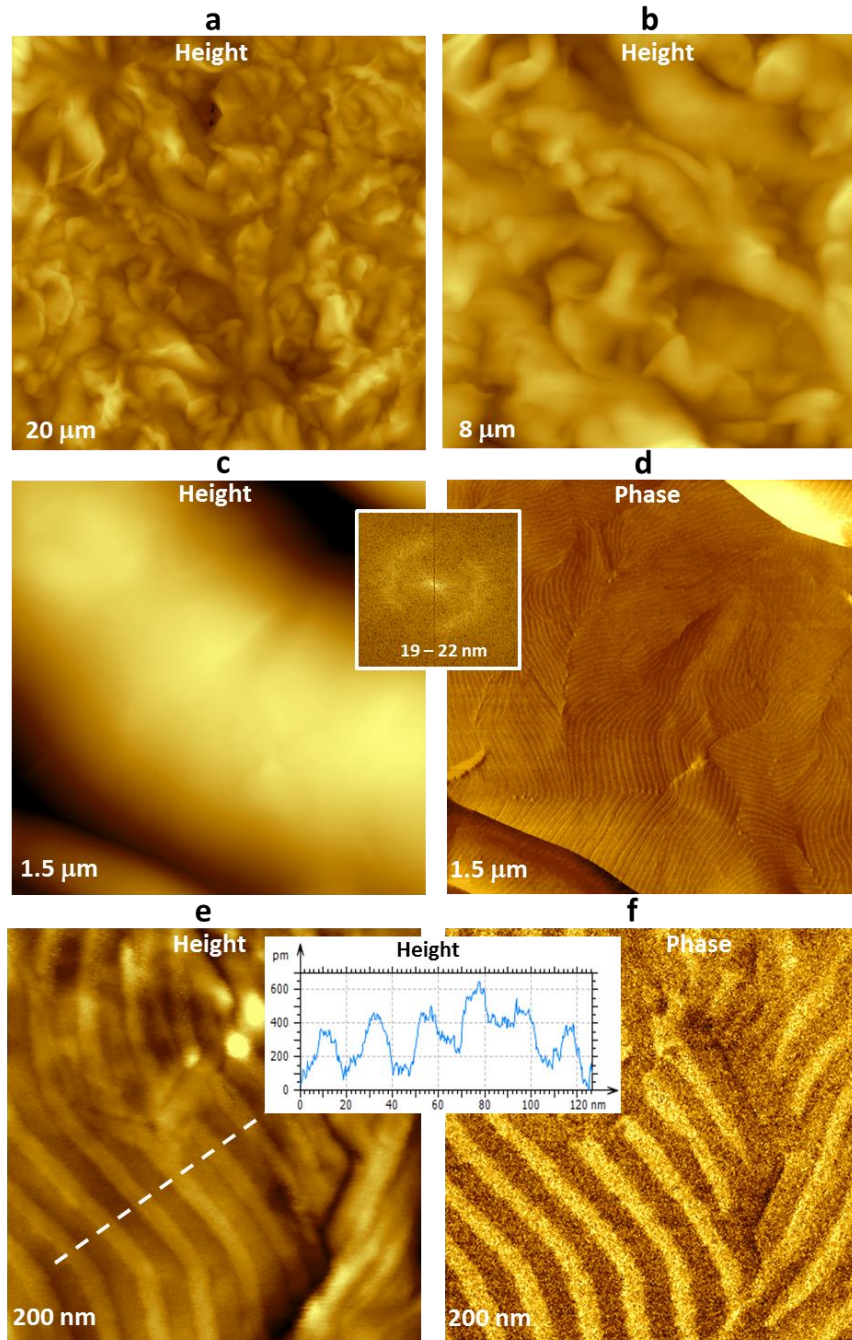


**Figure 9.** (a) – (f) Height and phase images of thick melt-crystallized film of F14H20 on Si substrate. The insert between (a) and (d) shows PSD plot of the image in (d) with the spacings' range. The insert between (e) and (f) shows the height cross-section, which was taken in (e) across the direction marked with a white dashed line in (e). The images were obtained in AM-PI mode using Si probe with  $k = 0.302 \text{ N/m}$  at  $A_0 = 10 \text{ nm}$  and  $A_{sp} = 6 \text{ nm}$ .

Surfaces of bulk samples of semi-fluorinated alkanes were examined early with TEM and optical microscopy [11]. Particularly, TEM micrographs of a replica taken from F12H20 sample have revealed periodical strips with 6 nm and 24 nm pitch. The small pitch was assigned to bilayer lamellar structures similar to those (6.5 nm) observed for F14H20 adsorbate in **Fig. 5f, 6d**. The structures related to 24 nm pitch were assigned to cylinders with uniform diameter. The proposed model of the cylinder suggests a concentric tubular lamellae arrangement melt crystallized material. AFM images of surface of bulk F14H20 alkane (**Fig. 9a-b**) reveal a corrugated morphology formed by short fibrils of different width and orientation and edged structures. One of fibrils with 1 micron in width is shown in **Fig. 9c**. The phase image in **Fig. 9d** reveals an ordered nanoscale pattern. Its main spacing, which was evaluated with PSD plot, varies in the 19-24 nm range. The images in **Fig. 9e** shows that height corrugations in the 300-400 pm range corresponding to the periodical surface features, whose alternation is consistent with the PSD data. The phase changes in **Fig. 9f** indicate a dissimilar nature of the neighboring regions in the periodical pattern that likely relates to variations of molecular packing.

## Conclusions

AFM studies of normal ( $C_{242}H_{486}$ ) and semifluorinated (F14H20) alkanes, which were deposited on HOPG and Si substrates by spin-casting and sublimation, have illustrated several important features of adsorbates' order and imaging of these structures in AM-PI mode. Epitaxial order of several layers of  $C_{242}H_{486}$  lamella on HOPG was observed on thin layers, which were prepared by spin casting and thermal treatment. This finding is similar to the results obtained earlier with short ( $C_{60}H_{122}$ ) [5] and ultra long  $C_{390}H_{782}$  [9] alkanes on this substrate. The analysis of AFM images of  $C_{242}H_{486}$  layers revealed that the interpretation of the height contrast requires a caution, particularly, when the surface corrugations are in the range of few nanometers or less. The imaging at small forces might be helpful in this respect. The other issue is visualization of weakly bonded surface structures, which were detected in the height images. A minimization of the tip force in AM-PI was not sufficient to record the top and less ordered material that was pushed around by the scanning probe. Therefore, to develop the imaging with small forces is one of the actual problems of this technique and, hopefully, progress will be made with PLL-based oscillatory techniques such as Amplitude Modulation with Frequency Imaging [12] and Frequency Modulation with Amplitude Imaging accompanied with the use of soft probes.

In addition to a more common spin-casting preparation, we applied a sublimation procedure as a solvent-free deposition of F14H20 compound on different substrates. In case of F14H20, whose adsorbates are very sensitive for solvent nature and environment, this approach helps to understand the role of the solvents and vapors in in formation and transformations of self-assemblies of this material. Variety of observed F14H20 self-assemblies has started with molecular layers whose spacings in AFM images are consistent with earlier X-ray data and can be explained by either tilted structure or the existence of double layered lamellae with indented hydrocarbon segments. The diversity of larger self-assemblies (ribbons, donuts, spirals) is common for adsorbates casted from different solvents, and similar ordered structures were observed in the sublimated deposits on different substrates. In other words, the intermolecular interactions of F14H20 material are the main governing factors in defining their self-assemblies. The self-assemblies were differentiated not only by their type but also by dimensions within one kind as seen in the images the ribbons' aggregate.

Another observation in AFM images of F14H20 lamellar layers was related to Moiré patterns. The pitch of superimposed periodical structure is generated by mixing the observed features with periodical scanning lines of imaging. The artifact can be recognized by changing a size of scanning area or image density. In case of F14H20 lamellar layers the true surface features of 6.5 nm apart were observed most clearly in the sub-micron imaging. This is not the only reason of Moiré patterns, which were registered in scanning tunneling and AFM images [13-14]. These effects can be caused by an overlayer of periodical structures with different orientation and the superposition arrangement shows up in the images due to local force variations.

## References

- [1] Q. Zhong, D. Innis, K. Kjoller, and V. Elings "Fractured polymer/silica fiber surface studied by tapping mode atomic force microscopy" *Surf. Sci. Lett.* **1993**, *290*, L688–L692.
- [2] S. Belikov, J. Alexander, C. Wall, and S. Magonov "Tip-sample forces in atomic force microscopy: interplay between theory and experiment" *Mater. Res. Soc. Symp. Proc.* **2013**, 1527-1532.
- [3] Y. Jiao, and T. E. Schäffer, "Accurate height and volume measurements on soft Samples with the atomic force microscope", *Langmuir*, **2004**, *20*, 10038–10045.
- [4] M. Bai, S. Trogisch, S. Magonov and H. Taub "Explanation and correction of false step heights in amplitude modulation atomic force microscopy measurements on alkane films" *Ultramicroscopy* **2008**, *108*, 946-952.
- [5] S. N. Magonov, and N. Yerina "High temperature atomic force microscopy of normal alkane C<sub>60</sub>H<sub>122</sub> films on graphite" *Langmuir* **2003**, *19*, 500–504.
- [6] A. Mourran, B. Tartsch, M. Galyamov, S. Magonov, D. Lambreva, B. I. Ostrovskii, I. P. Dolbnya, W. H. de Jeu, and M. Moeller "Self-assembly of the perfluoroalkyl-alkane F14H20 in ultrathin films" *Langmuir* **2005**, *21*, 2308–2316.
- [7] S. Magonov, J. Alexander, and S. Wu "Advancing characterization of materials with atomic force microscopy-based electric techniques" Ch. 9, pp. 233-300, in "Scanning probe Microscopy of Functional Materials: Nanoscale Imaging and Spectroscopy" (S. Kalinin, A. Gruverman, Eds.) Springer, **2011**.
- [8] J. Alexander, S. Belikov, S. Magonov, and M. Smith "Evaluation of AFM probes and instruments with dynamic cantilever calibrator" *MRS Advances* **2018**, 1-7 doi: 10.557/adv.2018.102
- [9] S. N. Magonov, N. A. Yerina, G. Ungar, D. H. Reneker, and D. A. Ivanov "Visualization of lamellae thickening during thermal annealing of single crystals of ultra long alkane (C<sub>390</sub>H<sub>782</sub>) and polyethylene" *Macromolecules* **2003**, *36*, 5637-5649.
- [10] T. P. Russell, J. F. Rabolt, R. J. Twieg, R. L. Siemens, and B. L. Farmer "Structural characterization of semifluorinated normal-alkanes. 2. Solid–solid transition behavior" *Macromolecules* **1986**, *19*, 1135–1143.
- [11] J. Hoepken, "Fluorocarbon-hydrocarbon molecules: structural components fir self-organizing components" PhD Thesis, University of Twente, **1991**.
- [12] S. Magonov, J. Alexander, M. Surtchev, A. Hung, and E. H. Fini "Compositional mapping of bitumen using local electrostatic force interactions in atomic force microscopy" *J. Microsc.* **2017**, *265*, 196-206.
- [13] S. N. Magonov, and M.-H. Whangbo, Surface analysis with STM and AFM: Experimental and theoretical aspects of image analysis" pp. 154-157. Weinheim, VCH, **1996**.
- [14] A. Y. Koyfman A. Y., S. N. Magonov, and N. O. Reich N. O. "Self-assembly of DNA arrays into multilayer sheets" *Langmuir* **2009**, *25*, 1091-1095.